TFE3-PD-L1 axis is pivotal for sunitinib resistance in clear cell renal cell carcinoma

Xudong Guo
Department of Urology, Shandong Provincial Hospital affiliated to Shandong First Medical University, Jinan, China

Ruxia Li
Department of Urology, Shandong Provincial Hospital affiliated to Shandong First Medical University, Jinan, China

Qiulei Bai
Department of Urology, Shandong Provincial Hospital affiliated to Shandong First Medical University, Jinan, China

Shaobo Jiang
Department of Urology, Shandong Provincial Hospital affiliated to Shandong First Medical University, Jinan, China

Hanbo Wang (wanghanbo0709@163.com)
Department of Urology, Shandong Provincial Hospital affiliated to Shandong First Medical University, Jinan, China https://orcid.org/0000-0002-6095-8611

Research

Keywords: clear cell renal cell carcinoma, TFE3, PD-L1, sunitinib

Posted Date: August 4th, 2020

DOI: https://doi.org/10.21203/rs.3.rs-49292/v1

Version of Record: A version of this preprint was published at Journal of Cellular and Molecular Medicine on November 3rd, 2020. See the published version at https://doi.org/10.1111/jcmm.16066.

Abstract

Background: The microphthalmia of bHLH-LZ transcription factors (MiT/TFE) family chromosomal translocation or overexpression is linked with a poor prognosis in clear cell renal cell carcinoma (ccRCC) with elevated recurrence and drug resistance, but the molecular mechanism is not fully understood. Here, we investigated whether the resistance to sunitinib malate (Sun), the standard treatment for metastatic RCC, is due to upregulation of programmed death ligand 1 (PD-L1) by the transcription factor E3 (TFE3) in ccRCC.

Methods: The effect of TFE3 expression on ccRCC proliferation had been evaluated. The regulation of TFE3 on PD-L1 was assessed by qPCR and western blots in human primary clear cell lines and ccRCC specimens. The regulation of Sun on TFE3 and PD-L1 was assessed by western blots and flow cytometry. The therapeutic efficacy of Sun plus PD-L1 blockade was evaluated in xenograft mouse model.

Results: In this study, we propose that TFE3 but not TFEB is essential for tumor survival and more importantly it is more of a promotor of cell proliferation which was associated with the poorer survival of cancer patients. We also found a positive correlation between TFE3 and PD-L1 expression in clear cell RCC cells and tissues. Sun treatment led to enhanced TFE3 nuclear translocation and PD-L1 expression. Finally, we observed the therapeutic benefit of Sun plus PD-L1 inhibition which enhanced CD8+ cytolytic activity and thus tumor suppression in a xenografted mouse model.

Conclusions: Our data provides a strong rationale to apply Sun and PD-L1 inhibition jointly as a novel immunotherapeutic approach for ccRCC treatment.

Background

Renal cell carcinoma (RCC) has become the most malignant tumor of kidneys in adults, corresponding to 3.7% of all adult cancers worldwide [1]. Clear cell renal cell carcinoma (ccRCC) is the most common subtype of RCCs, representing approximately 65–70% of all adult renal carcinomas. The other histologies mainly encompass papillary (20%) and chromophobe RCC (5%) [2]. The prognosis of RCC is poor: 30% of patients are metastatic at diagnosis and almost 30% of the remaining patients will develop metastasis detected during the follow-up [3]. The treatment and management of metastatic RCC have radically changed over the past 20 years [4]. Initially, first-generation immunotherapy with cytokines: interleukins or interferon represented standard approaches but with poor results [5, 6]. In recent years, the development of tyrosine kinase inhibitors (TKI), mainly targeted to vascular endothelial growth factor receptor, largely improved the prognosis of both overall survival (OS) and progression free survival (PFS) [7]. Sunitinib malate (Sun) is an oral multi-targeting tyrosine kinase inhibitor that is registered for the treatment of advanced or metastatic renal cell carcinoma [8, 9]. Currently, the emergence of immune checkpoint inhibitors (ICI) showed promising results in RCC treatment [10-12]. Cytotoxic T-lymphocyte-associated protein-4 (CTLA-4), programmed cell death 1 (PD-1) and programmed death ligand-1 (PD-L1) could inhibit the proliferation and differentiation of immunocompetent cells and the recognition of tumor cells by

tumor-infiltrating lymphocytes (TILs). Curently, PD-1/PD-L1 axis has attracted massive interest [13]. Blockade the PD-1/PD-L1 axis has been of benefit in the treatment of many different types of cancers including RCC [14, 15].

TKI or ICI for the treatment of RCC has significantly improved the OS, PFS and durable responses in some patients. However, resistance and relapse are common; and only 15–25% of patients exhibit clinical responses to checkpoint blocking when given as monotherapy [16, 17]. So, innovative combinations of TKI with ICI are now part of the treatment strategy and have achieved exciting benefits according to the results of recently updated phase III trials [10, 18, 19]. However, the molecular mechanisms of these novel combinations need further investigations.

The MiT-TFE family of basic helix-loop-helix leucine-zipper transcription factors including TFEB, TFE3, TFEC and MITF play a major role as regulators of lysosome biogenesis, cellular energy homeostasis, and immune responses, thus they were originally described as oncogenes [20]. The expression of the TFEB and TFE3 and their activity are elevated in multiple types of human cancers and associated with enhanced proliferation and motility of these cancer cells [21]. Furthermore, TFEB or TFE3 fusion and overexpression caused by chromosomal translocation events is linked with a poor prognosis in a subset of RCC patients with elevated recurrence and metastasis [22]. But the molecular mechanism is not fully understood. Recently, XP Yang, et al reported that TFEB mediates immune evasion and resistance to mTOR inhibition of renal cell carcinoma via induction of PD-L1 [23]. These studies have shown that the MiT-TFE family plays an important role not only in the progression, but also chemotherapy resistance of RCC tumors.

In this study, we found that TFE3 is also a potent tumor promotor just like TFEB in ccRCC. Importantly, TFE3 but not TFEB is essential for the survival of tumor cells. TFE3 can also regulate PD-L1 expression in ccRCC cell lines and primary human ccRCC tumor tissues. We also found that Sun enhanced TFE3 nuclear translocation and PD-L1 expression. Combination of Sun with anti-PD-L1 enhanced the therapeutic efficacy in a mouse RCC xenograft model. Thus, our data provides rationale for the combined use of Sun and PD-L1 blockade as a potential therapeutic strategy to treat ccRCC.

Materials And Methods

Cell culture and Reagents

786-O, A498, TK-10 ccRCC cells, Renca mouse RCC cell and HepG2 liver adenocarcinoma cell (the Cell Bank of the Chinese Academy of Sciences, Shanghai, China) were cultured in RPMI-1640 medium supplemented with 10% fetal bovine serum (HyClone) and 100 U/ml penicillin and 100 g/ml streptomycin. All these cells were routinely cultured in 5% CO_2 at 37 °C. After chemical treatments, cells were collected for western blots or other assays. Sunitinib malate (#S1042) was purchased from Selleck. Anti-mouse PD-L1 antibody (BP0101) was purchased from BioXCell.

Western blots analysis and antibody

Cells or tumor tissues were washed with ice-cold PBS and lysed in RIPA lysis buffer containing a fresh protease and phosphate inhibitor mixture (50 mg/ml aprotinin, 0.5 mM phenylmethanesulfonyl fluoride, 1 mM sodium orthovanadate, 10 mM sodium fluoride and 10 mM β-glycerolphosphate). Cell lysates were then prepared for western blots. Protein concentrations were quantified by BCA protein assay. Cell lysates were mixed with 4X loading buffer and heated at 95℃ for 5 min. Equal volumes of lysates were run on 5–15% SDS-PAGE gels and transferred to 0.2-mm nitrocellulose membranes (GE, A29411350). Blots were blocked for 1 h at room temperature in TBS with 0.05% Tween 20 (Sigma Aldrich, P7949) (TBS-T) and 5% nonfat milk. Primary antibodies were incubated overnight at 4℃ in TBS-T with 5% nonfat milk. HRP-conjugated secondary antibodies were incubated 1 h at room temperature. Blots were washed with TBS-T, 3 times, 5 min and TBS, 1 time, 5 min each after both primary and secondary antibody incubations. Blots were developed with Western Lighting Plus-ECL (Thermo, TK275827) and exposed in dark room. Blots were normalized to GAPDH or β-Actin loading controls. Blots were incubated with primary antibodies against GAPDH (Santa Cruz, Sc-32233), Histone H3 (Cell Signaling Tech, 4499), β-Actin (Santa Cruz, Sc-47778), TFEB (Cell Signaling Tech, 37785), TFE3 (Cell Signaling Tech, 14779), and PD-L1 (Abcam, ab213524) overnight at 4°C prior to being probed with the appropriate peroxide-conjugated secondary antibodies.

Real-time quantitative PCR

Total RNAs was extracted using an RNAiso plus kit (TaKaRa, Japan). Complementary DNA was synthesized through reverse transcription using ReverTra Ace qPCR RT Kit (TOYOBO, Japan). Quantitative PCR analysis of cDNA was performed with SYBRGreen reaction master mix on a Real-time PCR System (Eppendorf International, Germany). Target mRNA levels were normalized to the level obtained for GAPDH. Changes in transcript level were calculated using DD△Ct method. The primers used in this experiment were listed in Table 1

Table 1: Primer

Name (Human)	Forward primer	Reverse primer
TFE3	CCGTGTTCGTGCTGTTGGA	GCTCGTAGAAGCTGTCAGGAT
TFEB	CCAGAAGCGAGAGCTCACAGAT	TGTGATTGTCTTTCTTCTGCCG
CD80	TGCCTGACCTACTGCTTTGC	AGGGCGTACACTTTCCCTTC
CD86	CGACGTTTCCATCAGCTTGTC	CGCGTCTTGTCAGTTTCCAG
CD273	ACCAGTGTTCTGCGCCTAA	CCTGGGTTCCATCTGACTTTG
CD274	GGTAAGACCACCACCACCAAT	TGATTCTCAGTGTGCTGGTCAC
CD275	CGTCTTCTTGAACATGCGGG	TTTTCTCGCCGGTACTGACT
CD276	CTCACAGGAAGATGCTGCGT	CTGTGAGGCAGAACCACAGT
VTCN1	TCTGGGCATCCCAAGTTGAC	TCCGCCTTTTGATCTCCGATT
VISTA	ACGCCGTATTCCCTGTATGTC	TTGTAGAAGGTCACATCGTGC
CD155	AGGCTATAATTGGAGCACGACC	GGTTTGTCCACAGGACGGAT
CD270	CAAGGTGATCGTCTCCGTCC	TCTGTGGGTCAGTGGTTTGG
GAL3	ATAACCTGCCTTTGCCTGGG	AGCAATTCTGTTTGCATTGGGC
HMGB1	TATGGCAAAAGCGGACAAGG	CTTCGCAACATCACCAATGGA
CD70	GTCACTTGGGTGGGACGTA	CAGTATAGCCTGGGGTCCTG
CD154	ACATACAACCAAACTTCTCCCCG	GCAAAAAGTGCTGACCCAATCA
CD252	GAGCCCCTCTTCCAACTGAA	CAGTTCTCCGCCATTCACAT
β-ACTIN	CATGTACGTTGCTATCCAGGC	CTCCTTAATGTCACGCACGAT
GAPDH	GGAGCGAGATCCCTCCAAAAT	GCTGTTGTCATACTTCTCATG

xCELLigence

Experiments were carried out using the RTCADP instrument (Roche, Germany) which was placed in a humidified incubator maintained at 37°C with 5% CO2. For time-dependent cell response profiling, 10000 cells/well were added to 16 well E-Plates. The electronic sensors provided a continuous and quantitative measurement of cell index in each well. Cell index is a quantitative measure of cell number present in a well, e.g. lower cell index reflects fewer cells are attached to the electrodes. The E-Plate 16 was monitored over the time frame indicated.

ethynyl-2'-deoxyuridine (EdU) incorporation assay

EdU cell proliferation kit (17-10527) was purchased from Millipore (Massachusetts, USA). Pretreatment with siRNA, the cells were incubated 16 hours at 37℃ in complete media supplemented with 10 μmol/L EdU. After washing in PBS, the cells were fixed and permeabilized. Reaction cocktail and DAPI (Beyotime, Shanghai, China) were then added. The fluorescence change of cells was detected with flow cytometry or microscope.

Subcellular fractionation

Cells were lysed in NP-40 lysis buffer containing 20 mM Tris-HCL (pH 7.9), 150 mM NaCl, 0.5 mM EDTA and 0.5% NP-40 supplemented with protease and phosphatase inhibitors. Lysed cells were kept on ice for 15 min. The lysates were then centrifuged at 2,000 ×g for 5 min. The resulting supernatants represented the cytosolic and membrane fractions. The corresponding pellets representing the nuclear fractions were washed one time in NP-40-containing lysis buffer and sonicated in nuclear lysis buffer (20 mM Tris-HCl (pH 7.4), 450 mM NaCl, 0.5 mM EDTA, 0.5% Triton X-100, 0.1% SDS). The lysates were then centrifuged at 12,000 ×g for 15 min to obtain the cytosolic and nuclear fractions.

Microscopy

To measure TFE3 nuclear translocation, cells following TFE3-GFP transfection and Sun (5uM) treatments were incubated with DAPI for 10 min. The cells were then washed with PBS, and nuclear translocation fluorescence was measured using confocal microscopy (Carl Zeiss).

Patient samples

Clear cell renal cell carcinoma and benign samples were obtained from surgical excision specimens at the Shandong Provincial Hospital. Utilization of the clinical samples was approved by the Ethical Committee of the Shandong Provincial Hospital affiliated to Shandong First Medical University.

Immunohistochemistry (IHC)

Heat-induced epitope retrieval was performed in 10 mM citric acid buffer (pH 7.2) using a microwave. The slides were incubated at 4 °C overnight with primary antibodies (anti-PD-L1, 1:200 dilution; anti-TFE3, 1:200 dilution). An HRP-conjugated antibody and 3,30-diaminobenzidine (DAB) staining were used to visualize primary antibody binding. High-resolution pictures were obtained on a digital electron microscope, and images were recorded using Case Viewer software. Immunohistochemical results are expressed as a mean score that considers both the intensity of the staining and a positive reaction.

Transfection

Cells were transfected with specifically targeted TFEB (AGACGAAGGUUCAACAUCA), TFE3 (CGCAGGCGATTCAACATTAAC), and the plasmid of TFE3-GFP, using Lipofectamine 2000 Transfection Reagent.

Flow Cytometry

The PD-L1 expression in the cells were determined using flow cytometry. Cells following various treatments, were collected by centrifugation. After two washes with ice-cold PBS, Cells were stained with antibodies against PE-conjugated anti-human PD-L1 antibody. The antibodies used to stain tumor infiltrating lymphocytes (TILs) were listed as followed:anti-CD3-FITC (100203, Biolegend), anti-CD4-APC (100516, Biolegend), anti-CD8-Percp/Cy5.5 (100734, Biolegend), anti-GZMB-PE (104508, Biolegend).

Xenograft mouse tumor models

C57BL/6 mice (6 weeks old) were obtained from the Animal Center of the China Academy of Medical Sciences (Beijing, China). Murine RCC cell Ruca were injected into the right flanks of the mice and allowed to establish tumors. When the tumors reached 50~100 mm^3, the mice were given the clinical chemotherapeutics sunitinib (40 mg/kg, i.p.) daily, anti-PD-L1 (200 μg/mouse, i.p.). Tumor volumes (mm^3) were calculated from the formula $0.5 \times L \times W^2$ (L=length, W=width). All animal experiments were approved by the Ethics Committee of the Shandong University School of Medicine.

Statistical analysis

Western blots and fluorescent images were analyzed with Image Pro Plus 6.0. The data are presented as the mean ± SD and were analyzed with GraphPad Prism software (GraphPad). Student's t-test or one-way ANOVA was used for comparisons among different groups. Kaplan-Meier and Cox proportional hazards analyses were used for survival analysis. All the experiments were repeated at least three times. Values of $p<0.05$ denoted statistical significance and are indicated as $*p \leq 0.05$, $**p \leq 0.01$, and $***p \leq 0.001$ in the figures.

Results

TFE3 but not TFEB affects cell proliferation of ccRCC cells

The levels of TFEB and TFE3 are elevated in multiple types of human cancers and have been linked with both occurrence and poor prognosis [20-22, 24]. Recent study claimed that TFEB has little effect on RCC proliferation [23]. To clarify the role of TFEB and TFE3 in ccRCC, we first analyzed the publicly available Kaplan Meier plotter and The Cancer Genome Atlas (TCGA) database on the expression of TFEB and TFE3. As shown in Fig 1A, TFE3 but not TFEB was negatively correlated with the survival of patients in clear cell renal cell carcinoma. We also found that the basal expression of TFE3 is higher than that of TFEB in ccRCC specimens and tumor cell lines by TCGA and Cancer Cell Line Encyclopedia (CCLE) (Fig 1B). To further validate the database information, we examined 30 clinical renal clear cell carcinoma samples by qPCR and confirmed that TFE3 expression is higher (Fig 1C). To determine whether this difference defines the proliferative advantage of ccRCC, we tried to knockdown TFEB and TFE3 in 786-O cells (Fig 1D and E). As a result, knockdown of TFEB did not affect cell proliferation. This is consistent with previous report [23]. But interestingly, knockdown of TFE3 significantly inhibited cell proliferation (Fig 1F). These results were further validated by EdU staining and clone formation assay (Fig 1G-I). In addition, we also knocked down TFEB and TFE3 in hepatocellular carcinoma cells and got similar results (Supplementary Fig. 1A-D). This indicated that TFE3 can be at least another potent tumor promotor beyond TFEB in specifc tumor types such as ccRCC.

TFE3 mediates immune evasion by positively regulation the expression of PD-L1 in ccRCC cells and ccRCC patients

Recent study showed that TFEB can mediate immune evasion by positively regulation the expression of PD-L1 in RCC [23]. Encouraged by the similar roles of TFE3 and TFEB in the regulation of cell fate, we

next explored whether TFE3 also can mediate immune evasion by regulating the expression of immune checkpoint markers, such as PD-L1. As shown in Fig 2A, TFE3 and TFEB can both regulate the expression of some immune checkpoint markers, such as CD273 (PD-L2)、CD274 (PD-L1) and CD275 (ICOSL). To further clarify the regulation of TFE3 on the expression of PD-L1, we first down-regulated TFE3 and TFEB in multiple cells (A498, TK-10, HepG2) and then found that PD-L1 was down-regulated accordingly (Fig 2B). These results were further confirmed by western blots, immunofluorescence and flow cytometry (Fig 2C-F). We next evaluated whether the level of TFE3 correlated with PD-L1 expression in primary ccRCC patients. Within individual tumors, PD-L1 staining showed heterogeneous expression, which can be readily differentiated into PD-L1$^-$ and PD-L1$^+$ areas. Higher expression and enhanced nuclear localizations of TFE3 were seen in the PD-L1$^+$ regions (Fig. 3A-B). These results were further confirmed by western blots (Fig. 3C-D).

Sunitinib enhances PD-L1 expression via activation of TFE3 in ccRCC cells

Sunitinib is an oral tyrosine kinase inhibitor (TKI) that is currently registered for the treatment of advanced or metastatic renal cell carcinoma [8, 9]. Despite its initial excitement for the treatment of ccRCC, Sun rarely achieved complete responses and most patients ultimately developed resistance to Sun therapy, and the mechanism of resistance is not fully understood yet. Recent study reported that Sun increased PD-L1 expression in liver tumor cells [25]. Therefore, we proposed that the tolerance induced by Sun can also be related to the up-regulation of PD-L1 expression in ccRCC cells. As shown in Fig 4A-B, Sun (5μM) can induce the expression of PD-L1 in different ccRCC cells. These results were confirmed using flow cytometry of PD-L1 in 786-O cell (Fig. 4C). Given that TFE3 can regulate the expression of PD-L1 in our study, next we tried to see if Sun enhanced PD-L1 expression dependent of TFE3 expression. As shown in Fig 4D-E, Sun significantly enhanced TFE3 expression and its nuclear accumulation in 786-O cell. Knocking down TFE3 inhibited PD-L1 expression, and Sun-induced PD-L1 levels were also noticeably decreased in cells lacking of TFE3 (Fig. 4F-G). In contrast, the ectopic expression of TFE3 induced PD-L1 expression in the presence of Sun (Fig. 4H). Together, these data demonstrated that Sun can induce PD-L1 expression by activation of TFE3 in human ccRCC cells.

Anti-PD-L1 immunotherapy enhances the response to sunitinib in RCC

We then asked whether combined use of PD-L1 antibody could potentiate the efficacy of Sun on ccRCC growth in the xenograft mouse model. When tumor volume reached 50mm^3, mice were treated with either sunitinib (40 mg/kg, i.p.) daily, anti-PD-L1 (200 μg/mouse, i.p.) five times over 12 days, combination of both, or vehicle plus control IgG (Fig. 5A). There was a reduction in tumor growth in mice treated with either anti-PD-L1 alone or Sun alone compared to the control group (Fig.5B-D). By contrast the combination of Sun and anti-PD-L1 therapy resulted in a significant reduction in tumor size compared with all the other groups (Fig.5B-D). Next, we tested the effect of Sun and PD-L1 inhibition on cytotoxicity in tumor infiltrating CD8$^+$ T cells (CTL). Sun treatment suppressed GZMB expression in CTL, but when combined with anti-PD-L1, Sun significantly enhanced their expression (Fig. 5E). The combination

treatment also resulted in increased survival (Fig. 5F). Together, these data demonstrated that the combined use of Sun and anti-PD-L1 can be a novel immunotherapeutic approach for ccRCC treatment.

Discussion

Numerous studies have provided evidence suggesting that MiT/TFE transcription factors are important for the maintenance of cellular physiological and pathological processes [24]. Among all the four members of the MiT/TFE family, TFEB and TFE3 show a more ubiquitous pattern of expression and their functions has been widely investigated including proliferation, metabolism, and autophagy [20, 24]. The tight connection of TFEB and TFE3 with renal cell carcinoma has been reported, especially in translocation renal cell carcinoma (tRCC) [21-23]. But its biological function is not clearly investigated. We have found that the expression of TFE3 is higher than TFEB in tumor cells and patients. More interestingly, TFE3 but not TFEB has intrinsic effects on cell proliferation and survival in ccRCC and LIHC. This was consistent with the patient's prognosis. We also knocked down TFE3 and TFEB in lung cancer and breast cancer cells where their expression has no negative correlation with patient prognosis and it was found that alteration of the TFE3 or TFEB expression has little effect on tumor maintenance or progression (data not shown). These results suggest that TFE3 and TFEB are different in the regulation of biological processes, except for controlling autophagic and/or lysosomal function. And their specific molecular mechanisms need further study.

Identification the TFE3 regulated genes in ccRCC cells can provide better understanding of TFE3 functions in the regulation ccRCC tumorigenesis and the interaction between ccRCC cells and the immune microenvironment. Recent study showed that TFEB can mediate immune evasion by positively regulation the expression of PD-L1 in RCC [23]. Given the similar roles of TFE3 and TFEB in the cross-regulation of cellullar functions, we tested the expression of typical immune checkpoints, and interestingly we found that TFE3 can also regulate the expression of many immune checkpoints including CD273 (PD-L2)、CD274 (PD-L1)、CD275 (ICOSL) and CD270 (HVEM). Our study revealed a strong correlation between PD-L1 protein level and TFE3 expression in ccRCC cells and ccRCC patients.

Sunitinib is an oral tyrosine kinase inhibitor (TKI) that is currently registered for the treatment of advanced or metastatic renal cell carcinoma (RCC), gastrointestinal stromal tumor (GIST) and neuroendocrine tumor (NET) [8, 26, 27] Despite the early success of Sun on the treatment for ccRCC, most patients ultimately developed resistance whose mechanism is not fully understood. In fact, the resistance has been largely attributed to the derailing of intracellular signaling pathways, but less on the immune microenvirommment [8, 9]. In this study, we demonstrated that Sun led to enhanced translocation and expression of TFE3 in RCC cells, which subsequently induces PD-L1 expression. Furthermore, combination of Sun and anti-PD-L1 enhanced the cytotoxic functions of tumor infiltrating CTL and therapeutic efficacy in a mouse RCC xenograft model.

In summary, it is indicated that TFE3, like TFEB, is also a potent tumor promotor based on its significant proliferative effect. And more importantly, it mediates PD-L1 up-regulation, which can ultimately attenuate Sun therapeutic efficacy via tumor-associated immune-suppression. By emphasizing on the pivotal role

of TFE3, our data provides a valuable rational for the application of chemoimmunotherapy on the RCC patients.

Conclusions

Here, we find that TFE3 but not TFEB is essential for tumor survival and its proliferative effect was associated with the poor survival of cancer patients. A positive correlation between TFE3 and PD-L1 expression in clear cell RCC cells and tumor tissues. Sun treatment led to enhanced TFE3 nuclear translocation and PD-L1 expression. More importantly, sun plus PD-L1 inhibition which enhanced CD8+ cytolytic activity and tumor suppression in a xenografted mouse model of RCC. Thus, we present the newly discovered signal axis TFE3/PD-L1 in the sunitinib resistant human renal cell carcinoma. By emphasizing the importance of TFE3/PD-L1 axis, we hope this would provide a strong rationale to combine sunitinib and immune checkpoint inhibitors for future RCC treatment.

Abbreviations

RCC: renal cell carcinoma; Sun: Sunitinib malate; TFE3: The transcription factor E3; TFEB: The transcription factor EB; PD-L1: programmed death ligand 1; ccRCC: Clear cell renal cell carcinoma; TKI: tyrosine kinase inhibitors; OS: overall survival; PFS: progression free survival; CTLA-4: Cytotoxic T-lymphocyte-associated protein-4; PD-1:programmed cell death 1; IHC: Immunohistochemistry; TCGA: The Cancer Genome Atlas; CCLE: Cancer Cell Line Encyclopedia; GIST: gastrointestinal stromal tumor; NET: neuroendocrine tumor; CTL: cytotoxicity T cells; tRCC: translocation renal cell carcinoma.

Declarations

Acknowledgements and Funding

This work was supported by the Shandong Key Research and Development Program, China (2019GSF108263).

Authors' contributions

Xudong Guo performed most of experiments, analyzed data and organized figures and wrote the manuscript; Ruxia Li did qPCR analysis and the results shown in Fig. 2A and 2B; Qiulei Bai contributed to clinical samples collection and analyzed the clinical samples; Shaobo Jiang performed the study design, statistical analysis; Hanbo Wang supervised and designed the research work, analyzed and interpreted the data, revised and polished the manuscript.

Availability of data and materials

The datasets used and/or analyzed during the current study are available from the corresponding author on reasonable request.

Ethics approval and consent to participate

All procedures performed in studies involving human participants were following the ethical standards of the Ethics Committee of the Shandong First Medical University. All patients studied signed informed consent for participation. All animal procedures and care were conducted by institutional guidelines and in compliance with national and international laws and policies

Conflict of Interest Statement

None declare

Consent for publication

Not applicable.

References

1. Siegel RL, Miller KD, Jemal A: **Cancer statistics, 2019.** *CA Cancer J Clin* 2019, **69:**7-34.
2. Moch H, Cubilla AL, Humphrey PA, Reuter VE, Ulbright TM: **The 2016 WHO Classification of Tumours of the Urinary System and Male Genital Organs-Part A: Renal, Penile, and Testicular Tumours.** *Eur Urol* 2016, **70:**93-105.
3. Ljungberg B, Campbell SC, Choi HY, Jacqmin D, Lee JE, Weikert S, Kiemeney LA: **The epidemiology of renal cell carcinoma.** *Eur Urol* 2011, **60:**615-621.
4. Albiges L, Powles T, Staehler M, Bensalah K, Giles RH, Hora M, Kuczyk MA, Lam TB, Ljungberg B, Marconi L, et al: **Updated European Association of Urology Guidelines on Renal Cell Carcinoma: Immune Checkpoint Inhibition Is the New Backbone in First-line Treatment of Metastatic Clear-cell Renal Cell Carcinoma.** *Eur Urol* 2019, **76:**151-156.
5. Motzer RJ, Bacik J, Murphy BA, Russo P, Mazumdar M: **Interferon-alfa as a comparative treatment for clinical trials of new therapies against advanced renal cell carcinoma.** *J Clin Oncol* 2002, **20:**289-296.
6. Fyfe G, Fisher RI, Rosenberg SA, Sznol M, Parkinson DR, Louie AC: **Results of treatment of 255 patients with metastatic renal cell carcinoma who received high-dose recombinant interleukin-2 therapy.** *J Clin Oncol* 1995, **13:**688-696.
7. Motzer RJ, Hutson TE, Tomczak P, Michaelson MD, Bukowski RM, Rixe O, Oudard S, Negrier S, Szczylik C, Kim ST, et al: **Sunitinib versus interferon alfa in metastatic renal-cell carcinoma.** *N Engl J Med* 2007, **356:**115-124.
8. Rizzo M, Porta C: **Sunitinib in the treatment of renal cell carcinoma: an update on recent evidence.** *Ther Adv Urol* 2017, **9:**195-207.
9. Nassif E, Thibault C, Vano Y, Fournier L, Mauge L, Verkarre V, Timsit MO, Mejean A, Tartour E, Oudard S: **Sunitinib in kidney cancer: 10 years of experience and development.** *Expert Rev Anticancer Ther* 2017, **17:**129-142.

10. Motzer RJ, Tannir NM, McDermott DF, Aren Frontera O, Melichar B, Choueiri TK, Plimack ER, Barthelemy P, Porta C, George S, et al: **Nivolumab plus Ipilimumab versus Sunitinib in Advanced Renal-Cell Carcinoma.** *N Engl J Med* 2018, **378:**1277-1290.
11. Motzer RJ, Escudier B, McDermott DF, George S, Hammers HJ, Srinivas S, Tykodi SS, Sosman JA, Procopio G, Plimack ER, et al: **Nivolumab versus Everolimus in Advanced Renal-Cell Carcinoma.** *N Engl J Med* 2015, **373:**1803-1813.
12. Leite KR, Reis ST, Junior JP, Zerati M, Gomes Dde O, Camara-Lopes LH, Srougi M: **PD-L1 expression in renal cell carcinoma clear cell type is related to unfavorable prognosis.** *Diagn Pathol* 2015, **10:**189.
13. Wellenstein MD, de Visser KE: **Cancer-Cell-Intrinsic Mechanisms Shaping the Tumor Immune Landscape.** *Immunity* 2018, **48:**399-416.
14. Postow MA, Callahan MK, Wolchok JD: **Immune Checkpoint Blockade in Cancer Therapy.** *J Clin Oncol* 2015, **33:**1974-1982.
15. Weinstock M, McDermott D: **Targeting PD-1/PD-L1 in the treatment of metastatic renal cell carcinoma.** *Ther Adv Urol* 2015, **7:**365-377.
16. Chen Q, Xu L, Chen J, Yang Z, Liang C, Yang Y, Liu Z: **Tumor vasculature normalization by orally fed erlotinib to modulate the tumor microenvironment for enhanced cancer nanomedicine and immunotherapy.** *Biomaterials* 2017, **148:**69-80.
17. Gide TN, Quek C, Menzies AM, Tasker AT, Shang P, Holst J, Madore J, Lim SY, Velickovic R, Wongchenko M, et al: **Distinct Immune Cell Populations Define Response to Anti-PD-1 Monotherapy and Anti-PD-1/Anti-CTLA-4 Combined Therapy.** *Cancer Cell* 2019, **35:**238-255 e236.
18. Motzer RJ, Penkov K, Haanen J, Rini B, Albiges L, Campbell MT, Venugopal B, Kollmannsberger C, Negrier S, Uemura M, et al: **Avelumab plus Axitinib versus Sunitinib for Advanced Renal-Cell Carcinoma.** *N Engl J Med* 2019, **380:**1103-1115.
19. Rini BI, Plimack ER, Stus V, Gafanov R, Hawkins R, Nosov D, Pouliot F, Alekseev B, Soulieres D, Melichar B, et al: **Pembrolizumab plus Axitinib versus Sunitinib for Advanced Renal-Cell Carcinoma.** *N Engl J Med* 2019, **380:**1116-1127.
20. Raben N, Puertollano R: **TFEB and TFE3: Linking Lysosomes to Cellular Adaptation to Stress.** *Annu Rev Cell Dev Biol* 2016, **32:**255-278.
21. Zhang W, Li X, Wang S, Chen Y, Liu H: **Regulation of TFEB activity and its potential as a therapeutic target against kidney diseases.** *Cell Death Discov* 2020, **6:**32.
22. Kauffman EC, Ricketts CJ, Rais-Bahrami S, Yang Y, Merino MJ, Bottaro DP, Srinivasan R, Linehan WM: **Molecular genetics and cellular features of TFE3 and TFEB fusion kidney cancers.** *Nat Rev Urol* 2014, **11:**465-475.
23. Zhang C, Duan Y, Xia M, Dong Y, Chen Y, Zheng L, Chai S, Zhang Q, Wei Z, Liu N, et al: **TFEB Mediates Immune Evasion and Resistance to mTOR Inhibition of Renal Cell Carcinoma via Induction of PD-L1.** *Clin Cancer Res* 2019, **25:**6827-6838.
24. Yang M, Liu E, Tang L, Lei Y, Sun X, Hu J, Dong H, Yang SM, Gao M, Tang B: **Emerging roles and regulation of MiT/TFE transcriptional factors.** *Cell Commun Signal* 2018, **16:**31.

25. Li W, Zhan M, Quan YY, Wang H, Hua SN, Li Y, Zhang J, Lu L, Cui M: **Modulating the tumor immune microenvironment with sunitinib malate supports the rationale for combined treatment with immunotherapy.** *Int Immunopharmacol* 2020, **81:**106227.
26. Bracci R, Maccaroni E, Cascinu S: **Transient sunitinib resistance in gastrointestinal stromal tumors.** *N Engl J Med* 2013, **368:**2042-2043.
27. Marx A, Weis CA: **Sunitinib in thymic carcinoma: enigmas still unresolved.** *Lancet Oncol* 2015, **16:**124-125.

Figures

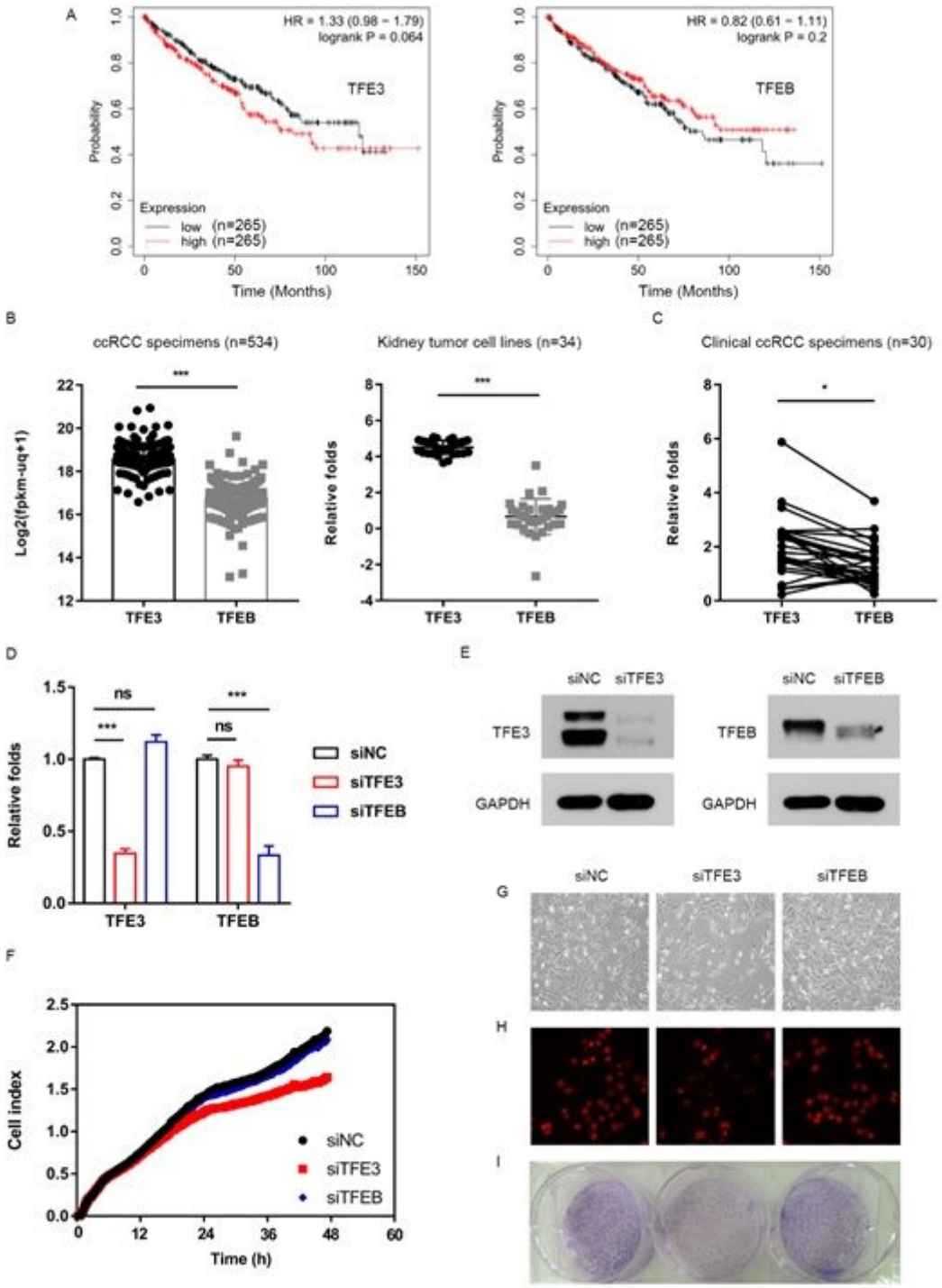

Figure 1

TFE3 but not TFEB affect cell proliferation of ccRCC cells (A) The relationship between TFE3/TFEB and patient prognosis in ccRCC was analyzed in data from Kaplan Meier plotter database. (B) The expression of TFE3 and TFEB in ccRCC specimens and RCC cells were analyzed in data from TCGA and CCLE database. (C) The expression of TFE3 and TFEB in ccRCC specimens was analyzed by qPCR. (D) siRNA knockdown of TFE3 and TFEB was analyzed by qPCR. (E) siRNA knockdown of TFE3 and TFEB was detected by western blots. (F) Cell viability was analyzed using a xCELLigence RTCADP instrument. (G) siRNA knockdown of TFE3 and TFEB was performed and the cell proliferation was analyzed by

morphology. (H) siRNA knockdown of TFE3 and TFEB was performed and the cell proliferation was analyzed by EdU. (I) siRNA knockdown of TFE3 and TFEB was performed and the cell proliferation was analyzed by clone formation. Data are mean ± SD, *P < 0.05, **P < 0.01 and ***P < 0.001.

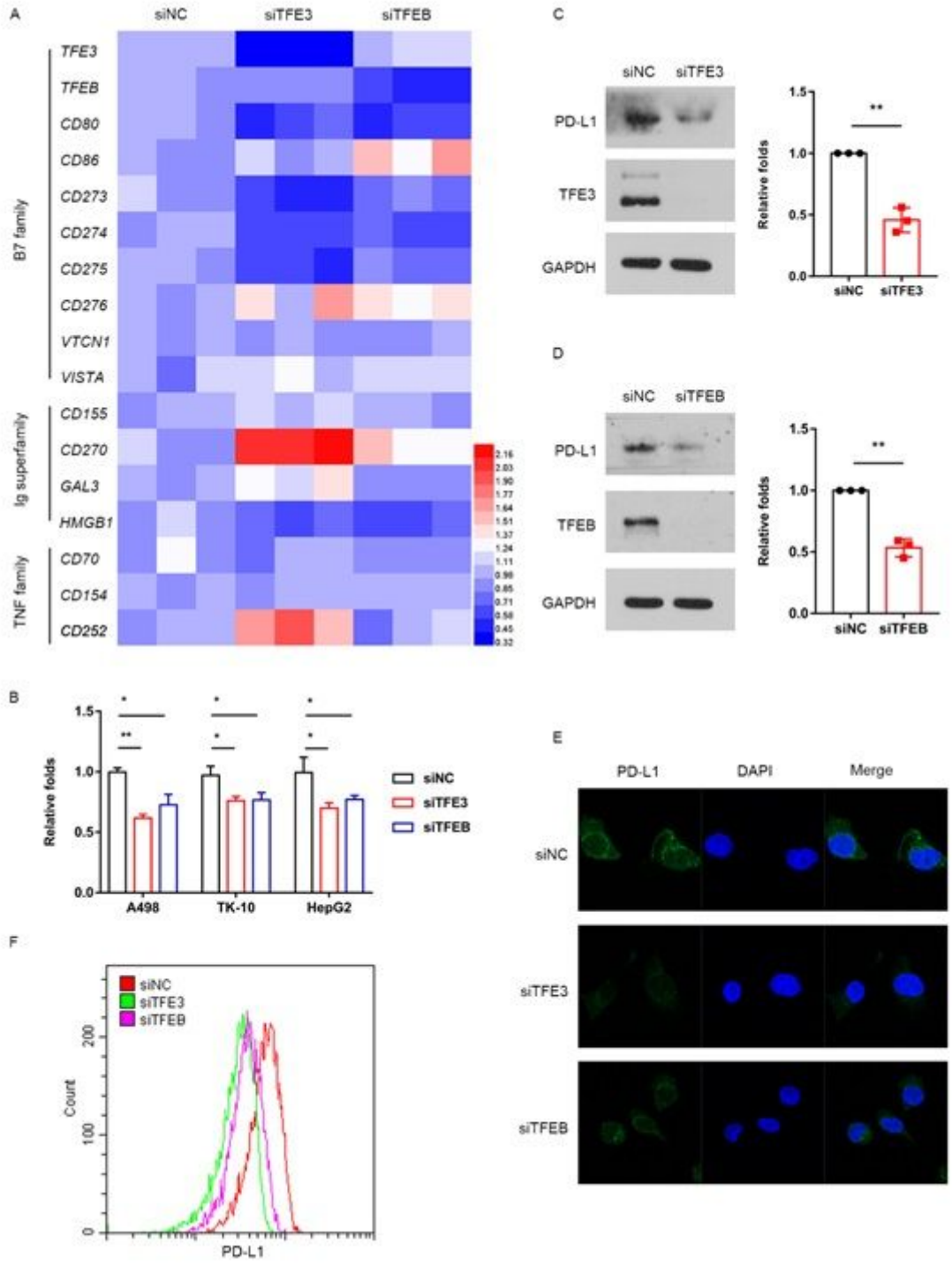

Figure 2

TFE3 mediates immune evasion by positively regulation the expression of PD-L1 in ccRCC cells and ccRCC patients (A) siRNA knockdown of TFE3 and TFEB was performed, and the heat map of immune checkpoints-related gene expression was analyzed by qPCR. (B) The expression of PD-L1 was analyzed by qPCR in multiple cells (A498, TK-10, HepG2). (C) TFE3 was knocked down with siRNA, and the

expression of PD-L1 was detected by western blots. (D) TFEB was knocked down with siRNA, and the expression of PD-L1 was detected by western blots. (E) TFE3 and TFEB were knocked down with siRNA, and the expression of PD-L1 was detected by immunofluorescent. (E) TFE3 and TFEB were knocked down with siRNA, and the expression of PD-L1 was detected by flow cytometry. Data are mean ± SD, *P < 0.05, **P < 0.01 and ***P < 0.001.

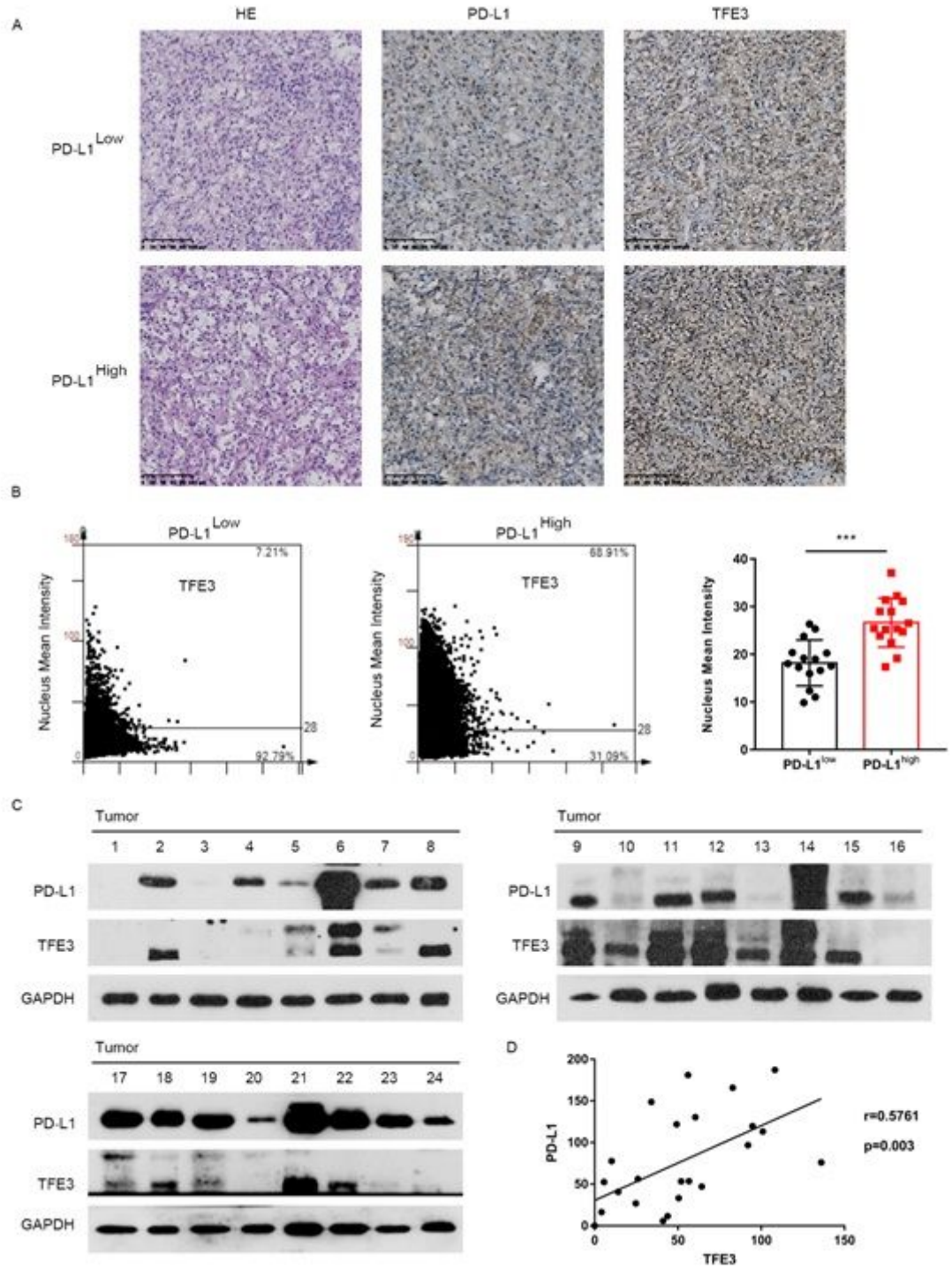

Figure 3

TFE3 mediates immune evasion by positively regulation the expression of PD-L1 in ccRCC cells and ccRCC patients (A) H&E and IHC staining with TFE3 and PD-L1 on human ccRCC tissues. (B) The nucleus

mean intensity of TFE3 in human PD-L1 negative and PD-L1 positive ccRCC tissues measured by IHC (n=30). (C) TFE3 and PD-L1 expression in ccRCC tissues were determined by western blots (n=24). (D) The correlation of TFE3 and PD-L1 expression in ccRCC tissues was plotted (n=24). Data are mean ± SD, *P < 0.05, **P < 0.01 and ***P < 0.001.

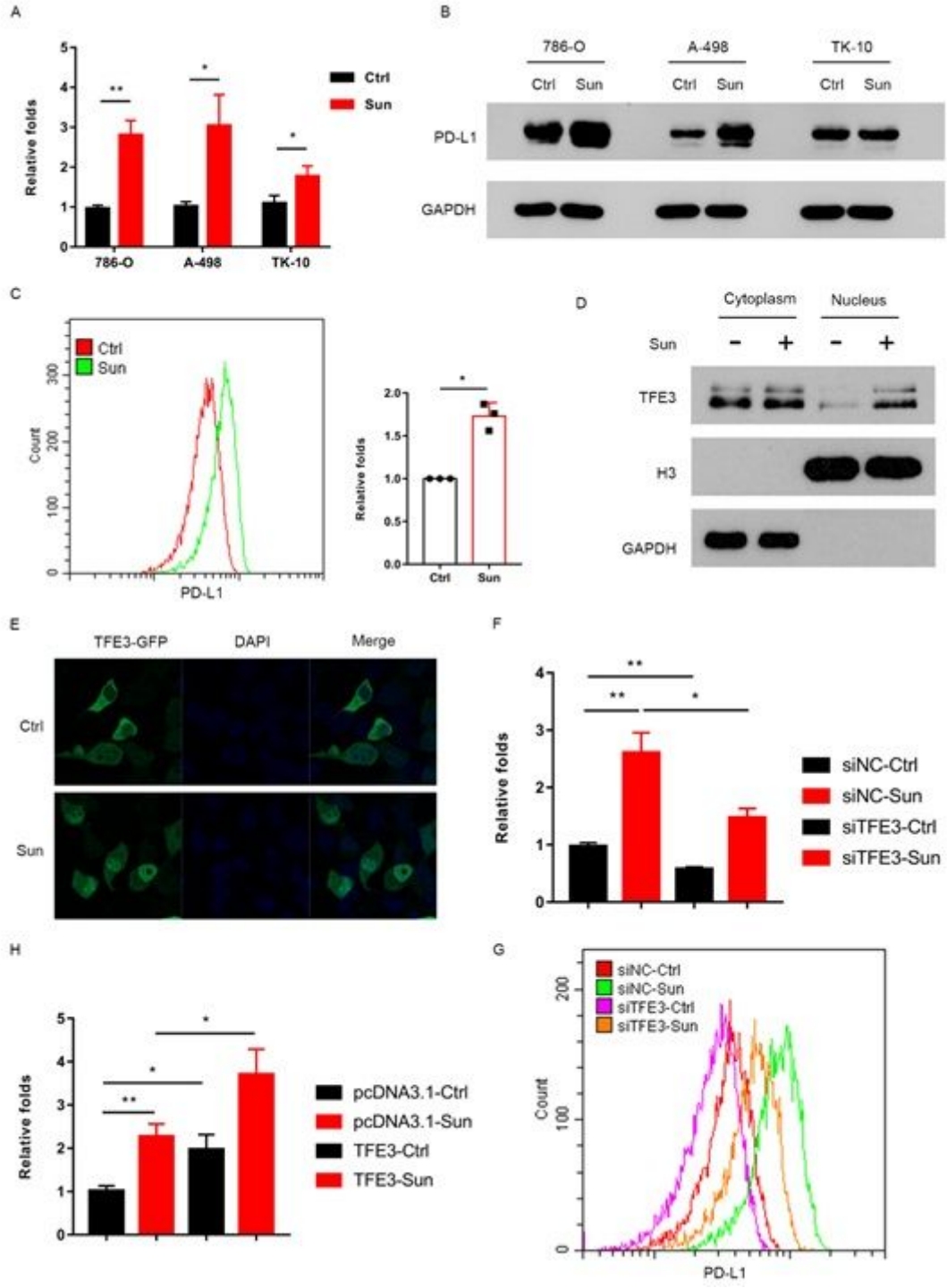

Figure 4

Sunitinib enhances PD-L1 expression via activation of TFE3 in ccRCC cells (A) PD-L1 expression was analyzed by qPCR in multiple cells (786-O, A498, TK-10) with sunitinib treatment. (B) PD-L1 expression was analyzed by western blots in multiple cells (786-O, A498, TK-10) with sunitinib treatment. (C) PD-L1

expression was analyzed by flow cytometry in 786-O cell with sunitinib treatment. (D) Western blots analysis of the nuclear translocation of TFE3 in 786-O cell with sunitinib treatment. (E) Immunoblots showing the TFE3 state in nuclear and cytosolic fractions of 786-O cell incubated with sunitinib. (F) siRNA knockdown of TFE3 was performed in combination with sunitinib treatment, and the expression of PD-L1 was analyzed by qPCR. (G) siRNA knockdown of TFE3 was performed in combination with sunitinib treatment, and the expression of PD-L1 was analyzed by flow cytometry. (H) Cells overexpressing TFE3 were treated with a combination of sunitinib, and the expression of PD-L1 was analyzed by qPCR. Data are mean ± SD, *P < 0.05, **P < 0.01 and ***P < 0.001.

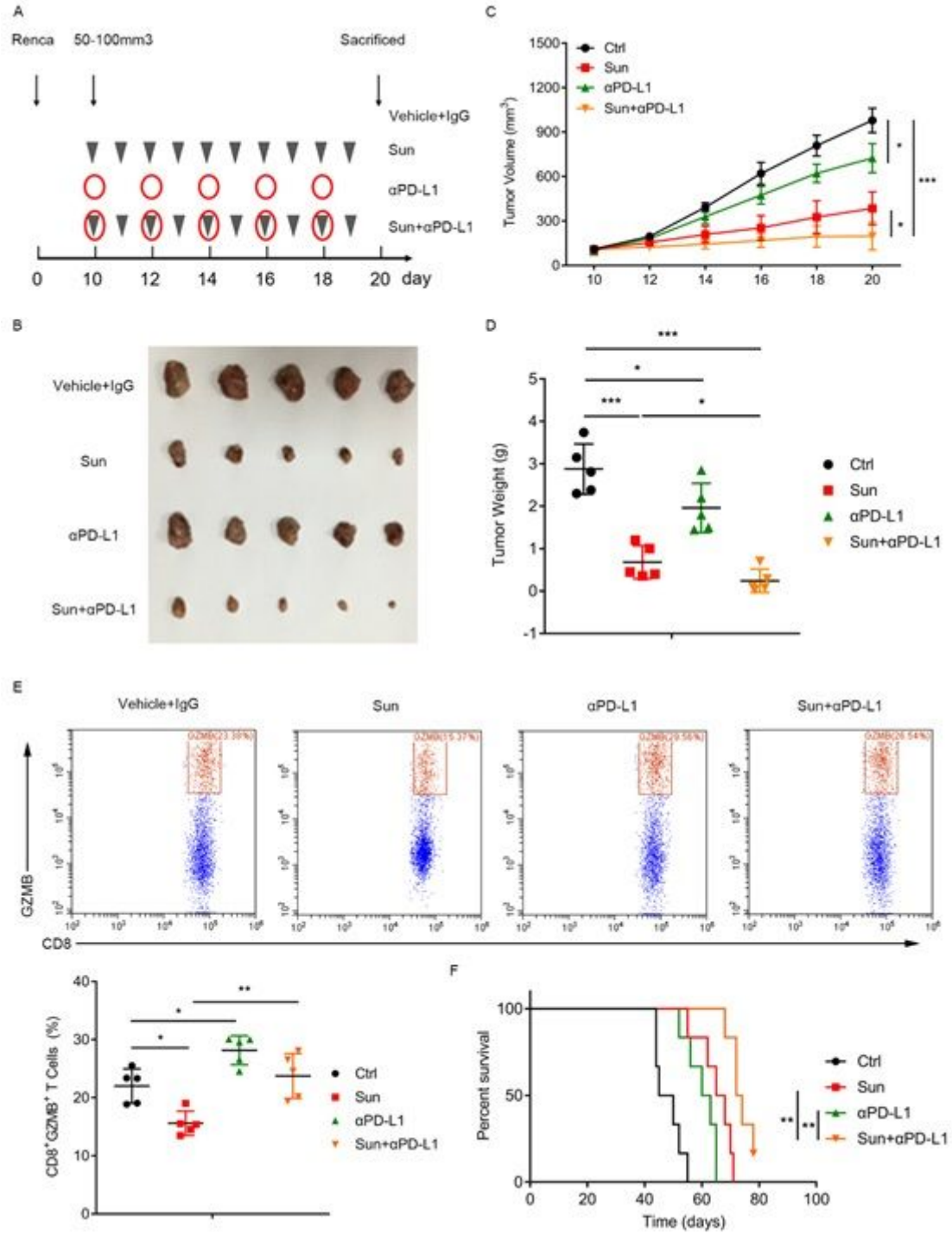

Figure 5

Anti-PD-L1 immunotherapy enhances the response to sunitinib in RCC (A) Model of the animal experiment. (B) Photographs of excised tumors from four groups (vehicle and IgG, sunitinib (40 mg/kg), anti-PD-L1(200 μg/mouse), or a combination of sunitinib and anti-PD-L1) are shown. (C) Tumor volumes in different groups were recorded every 2 days. (D) Tumor weights from four groups are shown. (E) TILs were isolated and stained with CD8 and GZMB. Representative histograms shown on the left panel. Percentages of CD8+ GZMB+ were shown on the right panel. (F) Homograft mice model showed overall survival difference from four groups. Data are mean ± SD, *P < 0.05, **P < 0.01 and ***P < 0.001.

Supplementary Files

This is a list of supplementary files associated with this preprint. Click to download.

- Supplementary.docx